2001 IEEE International Frequency Control Symposium and PDA Exhibition

RECOIL EFFECTS IN MICROWAVE ATOMIC FREQUENCY STANDARDS: PRELIMINARY RESULTS

Wolf P.[1], *Bize S., Clairon A., Landragin A., Laurent P., Lemonde P.*
BNM-LPTF/LHA, Observatoire de Paris

Bordé C.J.
Laboratoire de Physique des Lasers, Université Paris-Nord

Abstract

We investigate theoretically and by numerical simulations the effects of the atomic recoil on the frequency and fringe contrast of microwave atomic frequency standards. Such effects arise because of the influence of external degrees of freedom on the phases and the spatial positions of the interfering wave packets. We show under which conditions such effects lead to a frequency shift and examine the loss of contrast of the interference signal (Ramsey fringes). We use an interferometric description to model the frequency standards, treating simultaneously internal and external degrees of freedom [1]. We consider multiple momentum exchanges in 3D between the atoms and the standing microwave field inside the cavity leading to a large number of wave packets that leave the cavity with different momenta. At detection, these wave packets interfere giving rise to Ramsey fringes that are modulated by the interference of the external states of the wave packets. Similar treatments have proved efficient when treating 1D recoil effects in standing laser waves [2]. We apply this theoretical model numerically to laser cooled atomic fountain frequency standards and investigate the behaviour of the observed signal as a function of the frequency standard parameters (microwave power, launching height, etc.). Finally, we discuss possible experimental methods that could be used to observe such effects.

1. Introduction

In the last decade microwave atomic fountain frequency standards using laser cooled atoms have reached uncertainties of one part in 10^{15} [3] and are expected to improve by another order of magnitude in rubidium standards [4] and in space borne caesium standards [5], or even beyond that in optical frequency standards [2,6]. Paralleling that evolution atom interferometers have been successfully applied to other fields of metrology (gravimetry, gradiometry, gyroscopes) equalling or surpassing classical methods of measurements in those fields as well [7-9]. However, the two fields have to a large extent evolved separately although they rely essentially on the same principles. Indeed, while frequency standards have traditionally been described by the framework dating back to Ramsey [10] involving only the internal energy states of the atoms, atom interferometers on the other hand require descriptions that include the external motion and position states of the atoms. In fact any superposition of internal states goes hand in hand with a superposition of external states so a generic description of all these instruments (frequency standards, gravimeters, gyroscopes etc.) in terms of atom interferometry [1,11] should be of advantage to both fields. In this paper we apply such a description specifically to microwave frequency standards in order to investigate the effects of the external states of the atoms on the observed frequency and contrast of such standards.

Broadly speaking, any superposition of internal energy states of an atom induced by interactions with an electromagnetic field will give rise to a superposition of external states (external wave packets) whose momenta will differ by $\hbar\mathbf{k}$ (where $\hbar$ is Planck's constant and $\mathbf{k}$ is the wave vector of the electromagnetic field) due to the absorption of the photon momentum by the atom. The different external states will lead to additional energy differences (kinetic, potential). These will appear as a frequency shift of the standard as they add to the internal energy difference the standard is intended to measure. As an example, the kinetic energy difference due to the photon recoil is $(\hbar\mathbf{k})^2/2M$ (where M is the atomic mass) so the relative frequency shift in the case of a freely propagating wave ($k = \omega/c$) is

$$\frac{(\hbar k)^2}{2M}\frac{1}{\hbar\omega} = \frac{\hbar\omega}{2Mc^2} \qquad (1)$$

where c is the vacuum speed of light. For the hyperfine transition of caesium ($\omega \approx 5.8\ 10^{10}$ rad/s) this leads to a frequency shift of $\approx 1.5\ 10^{-16}$. Furthermore, it has been shown [2] that atoms interacting with standing electromagnetic waves (e.g. inside a microwave cavity) are subject to multiple photon processes, absorbing photons from one travelling wave component of the field and emitting them into another. This leads to final external states with total momenta $n\hbar k$ (where n is an

[1] on leave from Bureau International des Poids et Mesures (CNES research grant 793/00/CNES/8201)

0-7803-7028-7/01/$10.00 © 2001 IEEE

integer) so the order of magnitude of the shift obtained from (1) is likely to be only a lower limit of the total shift one might expect. These order of magnitude estimates are only a factor ten or less smaller than present frequency standard uncertainties, and of the same order as the uncertainties expected for the near future, which provides the motivation for the more detailed investigation presented in this work.

Another effect due to the separation of external states is a possible loss of contrast of the interference fringes (Ramsey fringes). Typically this will occur when the spatial separation of the interfering wave packets at detection is larger than some characteristic length of the atoms (atomic coherence length). The atomic wave packets separate at constant velocity (the recoil velocity, $v_r = \hbar k/M$) so this effect is likely to be more important for clocks with long drift times between the first interaction and detection, like fountain or space clocks.

We investigate both these effects describing the frequency standards as two zone atom interferometers. We model the atoms by Gaussian wave packets propagating freely (we neglect here gravitational, inertial and other external fields) through the interferometer, interacting with the microwave standing waves in the two interaction regions (cavities).

We first present the fundamental mathematical formalism required for the description of the atomic wave function and it's evolution, in free space and in the presence of the electromagnetic coupling field. In section 3 we apply this formalism to a simple, somewhat idealised, one dimensional, two zone standing wave interferometer. We then show how to apply the method to real microwave atomic frequency standards (section 4), with the results of a complete numerical simulation for a fountain standard given in section 5. We qualitatively explain the, somewhat surprising, results of that simulation in section 6 and conclude with a discussion of possible experimental observation of the predicted effects and of future perspectives on remaining theoretical work in section 7.

2. Fundamentals

We treat here a two level atom with ground and excited internal states $|g\rangle$ and $|e\rangle$ whose natural life-times are much longer than the characteristic times of the experiment. We therefore neglect any spontaneous emission processes and treat the electromagnetic field classically. The complete wave function of the atom can be expressed as a two component matrix

$$\Psi(t,z) = \begin{pmatrix} \Psi_e(t,z) \\ \Psi_g(t,z) \end{pmatrix}. \tag{2}$$

For simplicity we consider here only one spatial dimension, the generalisation to three dimension being straightforward.

The coupling field is

$$\mathbf{A}\, f(z)\cos(\omega t + \phi) \tag{3}$$

where **A** is the amplitude of the electric or magnetic field (depending on the interaction type), ω its angular frequency and ϕ an arbitrary initial phase. The function $f(z)$ describes the spatial form of the standing wave.

We assume a near resonant field and use the rotating wave approximation, neglecting off-resonant terms at frequencies 2ω, so the Schrödinger equation reduces to a pair of coupled equations

$$\begin{aligned} i\frac{\partial}{\partial t}\Psi_e(t,z) &= -\frac{\hbar}{2M}\frac{\partial^2}{\partial z^2}\Psi_e(t,z) + \frac{\Omega}{2}e^{-i\delta t} f(z)\Psi_g(t,z) \\ i\frac{\partial}{\partial t}\Psi_g(t,z) &= -\frac{\hbar}{2M}\frac{\partial^2}{\partial z^2}\Psi_g(t,z) + \frac{\Omega}{2}e^{i\delta t} f(z)\Psi_e(t,z) \end{aligned} \tag{4}$$

for free particles in the presence of the coupling field. Here M is the mass of the atom, $\delta = \omega - (E_e - E_g)/\hbar$ is the detuning and $\Omega = \langle e|\mathbf{D}_{op}\cdot\mathbf{A}_{op}|g\rangle/\hbar$ is the Rabi frequency with $\mathbf{A}_{op}$ the operator of the electric/magnetic field amplitude and $\mathbf{D}_{op}$ the appropriate atomic multipole operator depending on the interaction type (electric/magnetic dipole, quadrupole, etc.). For microwave frequency standards $\Omega \approx \mu_B B/\hbar$ where μ_B is the Bohr magneton and B is the amplitude of the magnetic field component parallel to the static magnetic field with $f(z)$ the spatial variation of that component. Note that (4) reduces to the simple free particle Schrödinger equation in the absence of the coupling field ($\Omega = 0$) and to standard Rabi equations for a two level system (see e.g. [12] equ. (10)) when neglecting the spatial dependence ($\Psi(t,z) \rightarrow \Psi(t)$ and $f(z) = 1$).

We will describe the external state of the atoms in terms of normalised Gaussian wave packets centred around a position z_0 at $t = 0$ and a velocity v_0:

$$\varphi(t,z) = N(t)\exp\left[\left(-P(t)+iQ(t)\right)\left(z-\left(z_0+v_0t\right)\right)^2\right]\exp\left[\frac{iM}{\hbar}\left(v_0\left(z-z_0\right)-\frac{v_0^{\,2}}{2}t\right)\right] \tag{5}$$

where the normalisation function in 1D is

$$N(t) = \frac{e^{-i\theta(t)}}{\left[2\pi\Delta^2\left(1+\frac{1}{\varepsilon}\right)\right]^{\frac{1}{4}}} \tag{6}$$

$$\mathrm{tg}(2\theta) = \frac{\hbar t}{2M\Delta^2} \tag{7}$$

and the functions describing the spreading of the wave packet and it's phase curvature are

$$P(t) = \frac{M^2\Delta^2}{\hbar^2 t^2(1+\varepsilon)} \tag{8}$$

$$Q(t) = \frac{M}{2\hbar t(1+\varepsilon)} \tag{9}$$

with ϵ defined as

$$\varepsilon = \frac{4M^2\Delta^4}{\hbar^2 t^2}. \tag{10}$$

The constant Δ will play a crucial role in the results presented in the following sections. It has the dimension of length and corresponds (as can be easily checked) to the half-width (in z) of the wave packet at the initial time t = 0. Physically, this corresponds to the half-width when the wave packet is minimal i.e. when $\Delta.\delta p = \hbar/2$, which is typically the case for atoms in the ground state of the cooling (Sysiphus) potential wells while the cooling is on. Therefore, we will set t = 0 at the end of the cooling phase, and approximate the atoms as Gaussian wave packets with some "mean" initial width Δ which depends in fact on the way the potential well eigenstates are populated during the cooling. Note that the parameter usually known in fountain clocks is the velocity distribution (temperature) of the atom cloud, but that this parameter has no simple direct relation to the width Δ, (Δ is, in general, not given by simply the Fourier transform of the velocity distribution). Indeed, the same velocity distribution can be obtained by a statistical ensemble of atoms in states with lower δv (large Δ) moving at different velocities or by an ensemble of atoms all in the same state (larger δv, all centred on the same v_0). Therefore the observed velocity distribution can only provide a lower limit on Δ (if it was smaller the observed velocity distribution would have to be larger even if all atoms were in the same state). As an example, for Cs atoms cooled to $\approx$ 0.8 μK ($\delta v \approx$ 7 mm/s) one obtains $\Delta \geq$ 34 nm.

3. Standing wave 1D interferometer

Consider an atom interacting with a one dimensional standing wave of form $f(z)$ = cos kz (sum of two counter-propagating travelling waves). The atom is initially in the ground internal state and at rest with respect to the standing wave. The field is pulsed in a sequence of two pulses, each of intensity and duration such that the probability of an atom being in the same internal state before and after the pulse is 0.5 (π/2 pulses). To change internal states the atom exchanges photons with each of the travelling wave components of the field, thereby also gaining or loosing momentum $\hbar k$. If the photon is absorbed from one of the waves and re-emitted into the other the final internal state is the same as the initial one but the wave packet has gained a total momentum of $2\hbar k$. The same process may repeat several times therefore each interaction leads to a multitude of external states (see fig. 1).

Formally, we need to solve the Schrödinger equation (4) with $f(z)$ = cos kz = ½(e^{ikz}+e^{-ikz}). To do so we first substitute

$$\Psi_e(t,z) = \sum_{a,n} e_n^a(t)\varphi_n^a(t,z)$$
$$\Psi_g(t,z) = \sum_{a,n} g_n^a(t)\varphi_n^a(t,z) \tag{11}$$

where a,n are integers and $\varphi^a_n(t,z)$ are normalised Gaussian wave packets (c.f. (5)) centred on velocities nv_r and positions av_rT at t=T_b (i.e. z_0 = av_rT - nv_rT_b in (5)), each multiplied by a complex coefficient $e^a_n(t)/g^a_n(t)$ that depends only on time. Substituting (11) into (4) we note that the resulting equations are satisfied if the $\Psi_{e/g}(t,z)$ are solutions of the free particle Schrödinger equation (which is of course the case for a linear superposition of Gaussians) and if

$$i\sum_{a,n}\dot{e}_n^a(t)\varphi_n^a(z,t) = \frac{\Omega}{4}e^{-i\delta t}\left(e^{ikz}+e^{-ikz}\right)\sum_{a,n} g_n^a(t)\varphi_n^a(z,t)$$
$$i\sum_{a,n}\dot{g}_n^a(t)\varphi_n^a(z,t) = \frac{\Omega}{4}e^{i\delta t}\left(e^{ikz}+e^{-ikz}\right)\sum_{a,n} e_n^a(t)\varphi_n^a(z,t) \tag{12}$$

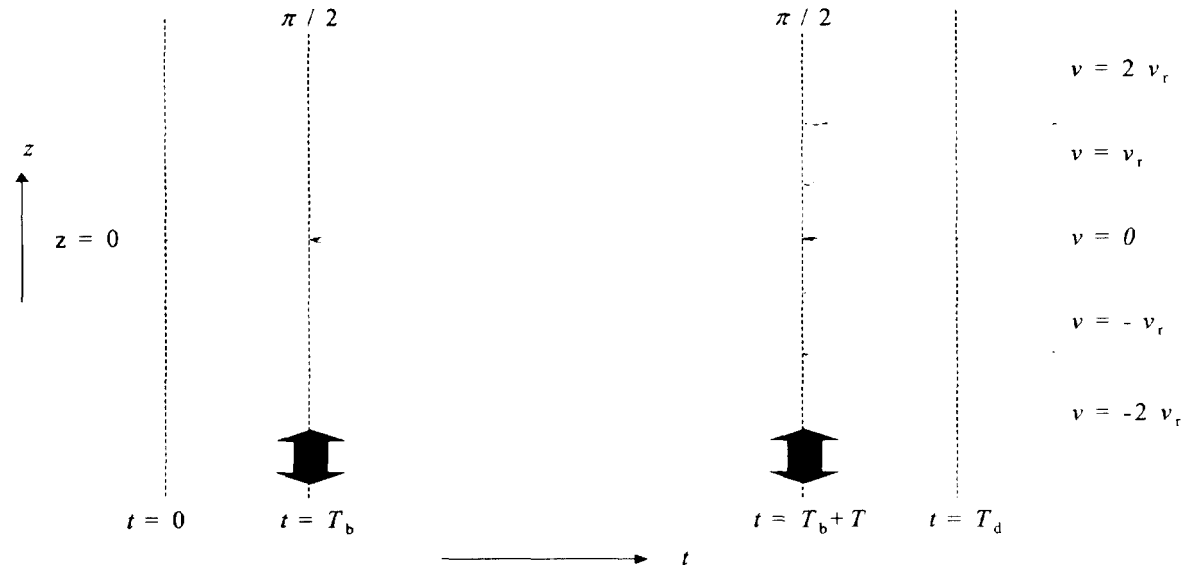

Figure1: Space-time picture of a two zone standing wave interferometer. The atomic wave packet centres follow the red (ground state) and green (excited state) lines. Initially (t=0) the atom is in the ground state and at rest at z=0. A first $\pi/2$ standing wave pulse is applied at $t=T_b$ and a second after a free evolution time T (at $t=T_b+T$). All ground (excited) wave packets interfere at detection ($t=T_d$).

For the first interaction $T_b-\tau/2 \le t \le T_b+\tau/2$ we start with a transformation

$$\breve{\varphi}_n^a(t,z) = \varphi_n^a(t,z)\exp\left[-\frac{iM}{\hbar}\frac{(nv_r)^2}{2}T_b\right]$$
$$\breve{e}_n^a/\breve{g}_n^a(t) = e_n^a/g_n^a(t)\exp\left[+\frac{iM}{\hbar}\frac{(nv_r)^2}{2}T_b\right] \quad (13)$$

We neglect the recoil kinetic energy and the movement of the wave packets during the interaction time τ (Raman-Nath approximation). This amounts to neglecting phase terms that are of order $M(nv_r)^2\tau/\hbar$ i.e. $\approx\tau/T$ smaller than the main recoil shifts accumulated during free propagation, and variations of the field over distances of order $v_r\tau$ (< 10^{-9} m for typical Cs fountain parameters). With this approximation it is easily seen (using (5) and transforming according to (13)) that during the interaction ($T_b-\tau/2 \le t \le T_b+\tau/2$) we have

$$\breve{\varphi}_n^a(t,z) \approx \breve{\varphi}_{n-1}^a(t,z)e^{ikz}. \quad (14)$$

Then, equating terms of identical $\breve{\varphi}_n^a(t,z)$, (12) reduces to an infinite set of coupled equations

$$i\dot{\breve{e}}_n^a(t) = \frac{\Omega}{4}e^{-i\delta t}\left(\breve{g}_{n-1}^a(t)+\breve{g}_{n+1}^a(t)\right)$$
$$i\dot{\breve{g}}_n^a(t) = \frac{\Omega}{4}e^{+i\delta t}\left(\breve{e}_{n-1}^a(t)+\breve{e}_{n+1}^a(t)\right) \quad (15)$$

The coefficient of each $\breve{\varphi}_n^a(t,z)$ is coupled to two others corresponding to the wave packets whose momenta differ by $\pm\hbar k$. The equations (15) model, of course, the multiple photon interactions taking place in the standing wave. Their solution provides the complete description of the quantum system after the interaction. The only initial non-zero coefficient is for $\breve{g}_0^0(t_0)=1$ which provides the initial conditions for the solution ($t_0 = T_b-\tau/2$).

For the resonant case (δ= 0) (15) has an analytical solution in terms of Bessel functions (c.f. [2, 13]). With the above initial conditions

$$\breve{e}_{2m+1}^0(t-t_0) = i(-1)^{m+1}J_{2m+1}\left(\tfrac{1}{2}\Omega(t-t_0)\right)$$
$$\breve{g}_{2m}^0(t-t_0) = (-1)^m J_{2m}\left(\tfrac{1}{2}\Omega(t-t_0)\right) \quad (16)$$

where the $J_m(x)$ are Bessel functions of the first kind and m is an integer running from -∞ to ∞. The probability to detect an atom in the excited state after the interaction is simply given by (neglecting again the separations and energies due to the external states and integrating over all z)

$$P_e(t_0+\tau) = \left|\sum_{n=-\infty}^{+\infty}\breve{e}_n^0(t_0+\tau)\right|^2 = \sin^2\left(\tfrac{1}{2}\Omega\tau\right) \quad (17)$$

where we have used (16) and standard identities of the Bessel functions (c.f. [13]). So Rabi oscillations are recovered, in particular a $\pi/2$ pulse ($\Omega\tau = \pi/2$) does

indeed correspond to a transition probability of 0.5. For off-resonant pulses ($\delta \neq 0$) (15) has to be solved numerically which, in general, raises no particular difficulties.

In the absence of the coupling field (between the two interactions) only the $\varphi^a_n(t,z)$ evolve, the coefficients $e^a_n(t)/g^a_n(t)$ remain unchanged (as can be easily seen from (12) when setting $\Omega = 0$).

The second interaction ($T_b+T-\tau/2 \leq t \leq T_b+T+\tau/2$) is treated in a similar way as the first one. We first transform, transferring phases accumulated during the free propagation (recoil energy) from the Gaussians $\varphi^a_n(t,z)$ to the coefficients $e^a_n(t)/g^a_n(t)$

$$\tilde{\varphi}^a_n(t,z) = \breve{\varphi}^a_n(t,z)\exp\left[\frac{iMv_r^2T}{\hbar}(na+n^2)\right]$$
$$\tilde{e}^a_n/\tilde{g}^a_n(t) = \breve{e}^a_n/\breve{g}^a_n(t)\exp\left[-\frac{iMv_r^2T}{\hbar}(na+n^2)\right] \quad (18)$$

The approximate relation (14) then becomes (under the same approximation)

$$\tilde{\varphi}^a_n(t,z) \approx \tilde{\varphi}^{a+1}_{n-1}(t,z)e^{ikz} \quad (19)$$

relating wave packets of different v_0 but same position at the second interaction ($t = T_b+T$). This leads to coupled equations analogous to (15)

$$i\dot{\tilde{e}}^a_n(t) = \frac{\Omega}{4}e^{-i\delta t}\left(\tilde{g}^{a+1}_{n-1}(t)+\tilde{g}^{a-1}_{n+1}(t)\right)$$
$$i\dot{\tilde{g}}^a_n(t) = \frac{\Omega}{4}e^{+i\delta t}\left(\tilde{e}^{a+1}_{n-1}(t)+\tilde{e}^{a-1}_{n+1}(t)\right) \quad (20)$$

which have to be solved once for each point at which one of the wave packets populated during the first interaction arrives(see Fig. 1).

Finally, the solutions of (15) and (20) provide the coefficients $e^a_n(T_d)/g^a_n(T_d)$ at the time of detection and the probability of detecting either one of the internal states is the result of the interference between all wave packets in that internal state at detection. For example, for the excited state

$$P_e(T_d) = \int_{\text{det.}} dz\left|\sum_{n,a} e^a_n(T_d)\varphi^a_n(T_d,z)\right|^2 \quad (21)$$

where the integral is taken over the spatial extension of the detection region.

As an aside, it can be noted that the case where the standing waves are replaced by travelling ones can be treated using the same formalism. Only the appropriate $e^{\pm ikz}$ are retained in (12) and as a result equations (15) and (20) reduce to only pairs (instead of infinite sets) of coupled equations. Those pairs of equations are, of course, standard Rabi equations with known analytical solutions [10,12] for all δ. Then using (21) for the detection (where the sums now involve only two wave packets for each internal state) one obtains expressions including the (single photon) recoil shift and the loss of contrast due to the separation of the wave packets (c.f. last paragraph of section 6).

4. Application to microwave standards

We consider here frequency standards with the interactions taking place inside microwave cavities of rectangular cross-section operating in the TE_{10} mode. The magnetic dipole atomic transitions are excited by the component of the magnetic field inside the cavity that is parallel to the static quantisation field. Then the form of the relevant standing wave inside the cavity is

$$f(\mathbf{r}) = \cos(\mathbf{k}_1\cdot\mathbf{r})\cos(\mathbf{k}_2\cdot\mathbf{r}). \quad (22)$$

With the cross-sectional plane in the x-z plane, $\mathbf{k}_1=(0,0,2\pi/\lambda_z)$ where the wavelength in the z direction (λ_z) is simply twice the z-dimension of the cavity and $\mathbf{k}_2=(0,2\pi/\lambda_g,0)$ where λ_g is the guide wavelength. The field is zero everywhere outside the cavity.

Consider first an atom at rest well inside the cavity with the field being pulsed for the two interactions (temporal case). The field is described correctly by (22) wherever atoms are present. The fact that the field is zero outside the cavity plays no role as the atoms do not "see" the zero field (mathematically, $f(z)$ only appears in the Schrödinger equation (4) in the product $f(z)\Psi(t,z)$ so its value in regions where $\Psi(t,z) = 0$ plays no role). This assumption remains true as long as the Gaussians in $\Psi(t,z)$ are significantly smaller than the size of the cavity (typically > 1 cm). The problem is then treated in the same way as in the previous section except that we substitute (22) into (4) (extended to 3D) writing it as

$$f(\mathbf{r}) = \frac{1}{4}\left(e^{i(\mathbf{k}_1+\mathbf{k}_2)\cdot\mathbf{r}}+e^{-i(\mathbf{k}_1+\mathbf{k}_2)\cdot\mathbf{r}}+e^{i(\mathbf{k}_1-\mathbf{k}_2)\cdot\mathbf{r}}+e^{-i(\mathbf{k}_1-\mathbf{k}_2)\cdot\mathbf{r}}\right) \quad (23)$$

so now four recoil directions are possible leading to external Gaussian states $\varphi^{ab}{}_{mn}(t,\mathbf{r})$ with their positions and velocities characterised by 2x2 matrices. This then leads to equations of form (15) and (20) for the first and second interactions where now each coefficient is coupled to four others. Finally the sum in (21) has to be extended over all four indices and the integral over the complete detection region in 3D.

In general, atomic frequency standards operate with the atoms moving through the two cavities (or twice the same one in fountain clocks), the microwave fields being

on permanently (spatial case). In that case the atoms "see" the transitions from (22) to zero field outside, i.e. during a short time (entrance and exit of the cavity) the atoms "see" a microwave field that is not correctly described by (22). Mathematically, over some time interval the atomic wave function overlaps with a field that is not correctly described by pure cosines and hence (23) is no longer correct.

One can approximate the spatial case by the temporal one, when neglecting these "transit effects" occurring when the atoms enter or exit the cavity (during the "transit times" when the atomic wave function is not completely outside or inside the cavity). This approximation is likely to hold as long as the atomic wave functions are much smaller than the dimensions of the cavity, as in that case the transit times will be much smaller than the total interaction time τ so the probability of absorbing or emitting a photon during transit is very small (even more so if the atoms cross the cavity parallel to $\mathbf{k}_1$, i.e. with field zeros at entrance and exit). For atomic fountain frequency standards this is likely the case for the first interaction (wave functions at least a factor 10 smaller than the cavities) but not necessarily for the second one. Quantifying precisely the effects of this approximation is part of the work still in progress (c.f. section 7).

Recently, the spatial case was treated rigorously in the weak field limit [14]. The results are consistent with those presented here (section 6). Further work to clarify the transition between the spatial and temporal cases is under way.

5. Numerical results

We numerically calculate the effect on the frequency shift and the contrast of the Ramsey fringes for a "typical" Cs atomic fountain standard using a rectangular cavity. The parameters of the modelled fountain are as follows: total time of flight of the atoms, T_d = 0.8 s (launching height ≈78 cm); time from the end of cooling to the first interaction, T_b = 0.15 s (cavity ≈47 cm above cooling region); time between the two interactions T = 0.5 s; size of detection region ≈ 1x1x30 cm. The size of the detection region is determined by the cross-section of the holes in the cavity (plus the small horizontal spreading of the wave packets between the second interaction and detection) and the time during which the detection beam is on ≈100 ms. The atoms are cooled to a temperature of 0.8 μK corresponding to a minimal value of $\Delta \geq 34$ nm. The cavity is a "standard" rectangular cavity with 22.86 mm x 10.16 mm cross-section which corresponds to k_1 = 137.43 m^{-1} and k_2 = 135.04 m^{-1}. The atoms cross the cavity along the vertical z direction parallel to $\mathbf{k}_1$.

We numerically solve the sets of coupled equations (15) and (20) for the case of four-fold coupling (c.f. (23)). We impose a cut-off number of total photon exchanges (number of recoils N_{rec}) determined by the required accuracy of the solution and the microwave power (for example, we use N_{rec} = 9 for $\pi/2$ pulses). One possible estimation of the accuracy of the solutions is to check that the total detection probability when taking into account only the coefficients $e(t)/g(t)$ (plane wave approximation) sums to 1, i.e.

$$P_e(t)+P_g(t)=\left|\sum_{a,b,m,n} e^{ab}_{mn}(t)\right|^2+\left|\sum_{a,b,m,n} g^{ab}_{mn}(t)\right|^2=1+\delta \tag{24}$$

where we generally obtain $\delta \approx 10^{-7}$ which corresponds to an error in the calculated frequency shift of $\leq 10^{-17}$ in relative value.

Table 1 gives the calculated relative frequency shift as a function of microwave power in the plane wave approximation ($P_e(T_d)$ and $P_g(T_d)$ defined as in(24)). The contrast is, of course, 100% in that case.

Power ($\Omega\tau$)	Shift ($\Delta\omega/\omega$)
$\pi/2$	2.4 10^{-16}
$3\pi/2$	-7.4 10^{-16}
$5\pi/2$	1.2 10^{-15}

Table 1: "Plane wave" frequency shift as a function of microwave power

As expected the shift is greater than the order of magnitude estimated using (1) (≈ 7.8 10^{-17} with $k \approx 137$ m^{-1} in the cavity) because of the population of external states at $n\nu_r$ due to multiple photon processes in the standing waves. Also the shift increases with microwave power as states with higher n get more populated. The change of sign can be easily understood qualitatively when one considers the states that are mainly populated for each value of $\Omega\tau$ and each internal state (c.f. the Bessel functions in (16)). For $\pi/2$ pulses the |g> state mainly populated is the initial state n=0 and the |e> state the one at n=±1. Hence the |e> states have (on average) higher kinetic energy than the |g> ones and the recoil shift is positive. On the other hand, for $3\pi/2$ pulses the |g> states mainly populated are those at n=±2 but the |e> states are still those at n=±1 so the situation inverses.

We then numerically integrate the complete sum of Gaussian wave functions of the atom over the detection region (c.f. (21)), obtaining the frequency shift and contrast of the Ramsey fringes.

Table 2. shows the frequency shift after integration of the atomic wave functions over the detection region ($P_e(T_d)$ and $P_g(T_d)$ defined as in (21)). The observables, $O_{e/g}$, actually used for the determination of the shift are normalised to the total detection probability (similar to the routine operation of Cs fountain clocks)

$$O_{e\ g}=\frac{P_{e\ g}(T_d)}{P_e(T_d)+P_g(T_d)}. \tag{25}$$

Δ [nm]	x-y [cm]	z [cm]	T_b [s]	$\Delta\omega/\omega$
34	1.2	30	0.15	$2.9\ 10^{-17}$
68	1.1	30	0.15	$8.8\ 10^{-18}$
34	1.2	0.2	0.15	$4.7\ 10^{-17}$
34	0.2	0.2	0.15	$5.6\ 10^{-17}$
34	1.2	30	0	$(< 10^{-18})$

Table 2: Frequency shift for Gaussian wave packets. The value in brackets is consistent with 0 when taking into account the estimated uncertainties of the numerical calculation.

All shifts are calculated for $\pi/2$ pulses and given as a function of the initial width of the wave packets (Δ) and of the size of the detection region in the horizontal plane (size of the square in the x-y plane) and in the vertical (z) direction. The last line corresponds to the special case where the cooling region is directly below the cavity (T_b = 0) which is interesting from a theoretical point of view (see section 6).

It is surprising that the calculated frequency shifts are about an order of magnitude smaller than the ones calculated in the plane wave approximation (c.f. table 1) or from the simple order of magnitude estimation (1). Understanding these results is more complex and treated in detail in section 6.

Table 3 gives the calculated contrast, C, of the interference (Ramsey) fringes. The contrast is simply the difference between the observables O_e and O_g (c.f. (25)) at resonance ($\delta = 0$), i.e.

$$C = \frac{\left|P_e(T_d) - P_g(T_d)\right|}{P_e(T_d) + P_g(T_d)}. \qquad (26)$$

$\Omega\tau$	Δ [nm]	x-y [cm]	z [cm]	C
$\pi/2$	34	1.2	30	0.876
π	34	1.2	30	0.639
$3\pi/2$	34	1.2	30	0.444
$\pi/2$	68	1.1	30	0.983
$\pi/2$	136	1.1	30	0.998
$\pi/2$	34	1.2	0.2	0.990
$\pi/2$	34	0.2	0.2	1.000

Table 3: Contrast for Gaussian wave packets.

Obviously one does not expect to see Ramsey fringes for π pulses. Nonetheless the quantity C as defined in (26) is of interest as it can be observed and is affected by the loss of coherence due to the separation of the wave packets at detection.

One expects the contrast to decrease as the separation of the wave packets increases beyond some characteristic length (atomic coherence length). This is indeed observed in the first three lines of table 3 (increased microwave power corresponds to larger separations as states at multiples of v_r get more populated). On the other hand, increasing the coherence length should increase the contrast. This is also observed in our simulation when increasing Δ, so Δ plays a role similar to a coherence length (see also section 6). As is well known from Gaussian optics, reducing the detection region also leads to a recovery of the interference contrast. This is confirmed in the last two lines of table 3.

It should be noted that all results obtained here are, strictly speaking, only valid for the case of a single atom described by a Gaussian wave function. For a statistical ensemble of such atoms some of the results may not, or only partly, apply. A detailed modelling of that case may be the subject of future work (c.f. section 7).

6. Qualitative understanding

To reach a qualitative understanding of the results presented in the previous section we will return to the 1D picture of section 3 (fig. 1) and consider the weak field limit i.e. reduced microwave power so that all interactions involving more than one recoil in each interaction zone can be neglected. We will look at the detection probability for the excited state, so only four wave packets interfere at detection: $e_1^{\,0}\varphi_1^{\,0}$, $e_1^{\,-1}\varphi_1^{\,-1}$, $e_{-1}^{\,1}\varphi_{-1}^{\,1}$, and $e_{-1}^{\,0}\varphi_{-1}^{\,0}$ which we will re-name for notational simplicity θ_1, θ_2, θ_3,and θ_4 (see fig. 2). Furthermore, we will assume that the detection region is much larger than the width of the wave packets at detection so the integral (21) can be extended from $-\infty$ to ∞.

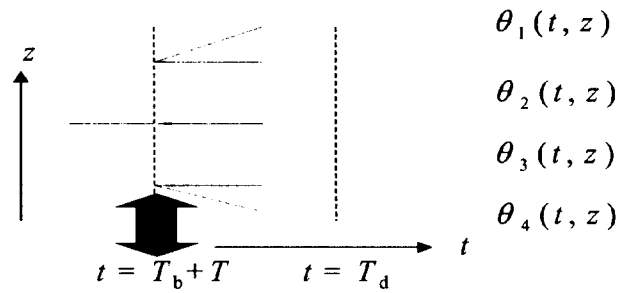

Fig. 2: Excited state wave packets at detection in the weak field approximation.

Then the probability (21) of detecting an atom in the excited state is

$$\int_{-\infty}^{\infty} dz \left[\sum_{j=1}^{4} A_j^2 + \sum_{j=1}^{4} \sum_{k \neq j} A_j A_k \cos(\phi_j - \phi_k) \right] \qquad (27)$$

where the A_j and ϕ_j are real functions of T_d and z representing the amplitude and phase of the complex wave functions $\theta_j(T_d,z) = A_j(T_d,z)\exp[i\phi_j(T_d,z)]$.

Of the interference terms in the double sum of (27) only those that were in different internal states during time T will be dependent on the detuning δ, and can therefore lead to a frequency shift of the Ramsey fringes. They are given by

$$\int_{-\infty}^{\infty} dz \begin{bmatrix} 2[A_1 A_2 \cos(\phi_1 - \phi_2) + A_4 A_3 \cos(\phi_4 - \phi_3)] \\ +2[A_1 A_3 \cos(\phi_1 - \phi_3) + A_4 A_2 \cos(\phi_4 - \phi_2)] \end{bmatrix} \tag{28}$$

where, by symmetry, the two terms inside each bracket are identical.

Before evaluating (28) rigorously we will try to estimate physically the content of the two phase differences ϕ_1-ϕ_2 and ϕ_1-ϕ_3. They are both affected by the phase difference due to the detuning δT and by the recoil energy difference $Mv_r^2T/2$. However, θ_1 and θ_3 have a momentum difference $2\hbar k/M$ which leads to an additional z-dependent phase term not present in the interference between θ_1 and θ_2. From these arguments one expects

$$\begin{aligned} \phi_1 - \phi_2 &\propto \delta T - \frac{\hbar k^2}{2M} T \\ \phi_1 - \phi_3 &\propto \delta T - \frac{\hbar k^2}{2M} T + 2kz \end{aligned} \tag{29}$$

When integrating the cosines over all z the z-dependent term in (29) averages to 0, however, for Gaussian wave packets the integral is effectively limited to the width of the Gaussians. In our case this is of the same order as the microwave wavelength associated with k so the additional term may play a non-negligible role. To estimate this, we simply choose a "reasonable" value for z in (29), for example, the midpoint between the two interacting wave packets θ_1 and θ_3, z = $\hbar kT/2M$. Then the total phase shift in the second bracket of (28) is $\delta T+\hbar k^2T/2M$ and the two cosines simply add to $2\cos(\delta T)\cos(\hbar k^2T/2M)$ which is consistent with zero shift. So the cancellation of the recoil shift is the result of the coherence between external states of opposing recoil directions that does not average on detection because of the comparable size of the atomic wave packets and the microwave wavelength. In fact, as we will show in the rigorous treatment below, the criteria for cancellation requires that the initial size of the wave packets Δ (rather than the size of the wave packet at detection) be much smaller than the wavelength of the standing wave.

We can find a rigorous expression for (28) by substituting for the amplitudes and phases from the corresponding Gaussian wave packets (c.f. (5)), bearing in mind that the two complex coefficients $e_{\pm 1}^{0}(T_d)$ (in θ_1 and θ_4) have a phase difference of δT - $\hbar k^2T/2M$ with respect to the other two $e_{\pm 1}^{\mp 1}(T_d)$ (in θ_2 and θ_3) due to the internal and kinetic energy difference during the time T between the two interactions (mathematically this is the result of the δ terms in (20) and the phases in the transformation (18)). The integrals of the resulting functions have known analytical solutions. After some simplification, and expanding in terms of the small parameter ε (c.f. (10), for Δ=34 nm $\varepsilon \approx 10^{-10}$) we obtain for the δ dependent interference terms

$$\propto \exp\left\{-\frac{v_r^2 T^2}{8\Delta^2}\right\} \left[\begin{aligned} &\cos\left(\delta T - \frac{\hbar k^2}{2M}\right) + \cos\left(\delta T + \frac{\hbar k^2}{2M}\right) \\ &\times \exp\left\{-\left(2\Delta^2 k^2 + \frac{\hbar^2 k^2 T_b (T_b + T)}{2M^2 \Delta^2}\right)\right\} \end{aligned} \right] \tag{30}$$

The first exponential in (30) simply describes the loss of coherence for separated wave packets (sometimes called a visibility function) and is responsible for the contrast observed in the numerical simulation (table 3). The two cosine interference terms add to $2\cos(\delta T)\cos(\hbar k^2T/2M)$ (consistent with 0 frequency shift) when the exponential factor of the second term is equal to one. For the parameters used in section 5 we obtain $\approx 10^{-10}$ and ≈ 0.25 for the first and second term inside the exponential respectively, so we expect some cancellation of the plane wave recoil shift as observed when comparing tables 1 and 2 of section 5. The second term in the exponential is dominant so we expect that for increasing Δ the observed shift decreases, as is indeed the case (table 2). In the special case of $T_b = 0$ we expect near zero shift (the second term in the exponential is 0) which is in agreement with the last line of table 2.

For arbitrarily small T_b the recoil shift will no longer cancel when the $2\Delta^2k^2$ term in the exponential is no longer << 1, which corresponds to the case when the wavelength of the standing wave is of the same order or smaller than the initial width of the wave packets (atomic coherence length). This is consistent with the idea that, in that case, the z dependent phase term in (29) averages to 0 over the atomic width.

Note that (30) can only provide a qualitative explanation of the results of the simulations (section 5) or of experiments, due to the fact that all external states at multiples of v_r are neglected, that only 1D recoils are taken into account, and that the detection is extended over all space rather than the actual detection region.

As an aside, when using travelling waves instead of standing ones (c.f. last paragraph of section 3) one obtains an interference term identical to (30) without the second cosine term. The well known recoil shift obtained in general from a plane wave treatment (e.g. [12]) is recovered but additionally the Gaussian treatment provides access to the loss of contrast related to the separation of the atoms.

7. Conclusion

We have presented detailed calculations of the frequency shift and contrast loss of the interference

(Ramsey) fringes in microwave atomic frequency standards due to the external states of the atomic wave packets. Depending on the experimental conditions the predicted frequency shift is of the order of a few parts in 10^{17} or less. This is an order of magnitude smaller than expected from order of magnitude estimates or calculations using a "plane wave" approach. We have qualitatively explained this surprising result, showing that it arises from the coherence between external states of opposing recoil directions that does not average on detection because of the small size of the atomic wave packets when compared to the microwave wavelength. We have derived explicit conditions (equ. (30)) under which such "cancellation" of the recoil shift occurs.

It is interesting to note that both main results obtained here (partial cancellation of the recoil shift and contrast loss) are not accessible to the plane wave approach used in most theoretical treatments on atom interferometry (e.g. [12,15]). Indeed, plane wave treatments reach their limits when a loss of contrast, or interference between wave packets with differing velocities and/or positions become important. In such situations approaches based on localised wave packets (e.g. Gaussians), like the one developed by Bordé and co-workers [14,16], have to be used.

The prediction that the recoil shift in microwave atomic frequency standards should not exceed a few parts in 10^{17} (although a plane wave approach or order of magnitude estimates indicate a shift $>10^{-16}$) is of particular importance to the uncertainty evaluation of the next generation of standards (Rb fountains and space Cs clocks) which are expected to reach uncertainties of one part in 10^{16} or less. This prediction is based on the theory presented here which is only a first approach that needs to be further studied (see below). Nonetheless, some experimental investigation may already be accessible with present technology. In particular the predicted loss of contrast (table 3) and its variation with experimental parameters (microwave power, launching height, etc.) may well be observable in present day atomic fountain standards when equipped with a rectangular cavity. Such experiments could verify the predictions presented here and thereby clarify whether the recoil shift can be neglected in the frequency evaluation of future standards.

Additionally such experiments will allow the investigation of the atomic density matrix (the ensemble of atomic wave functions) of a cold thermal cloud of atoms. In particular, some information on the coherence length of such a system may be obtained which is of prime importance for all atom interferometry experiments. For example, future space clocks that intend to take advantage of long drift times between the interaction zones may be subject to a significant loss of coherence due to the large separation of the wave packets at detection. In that case they would be ideal experiments to probe in more detail the quantum nature of the cold atom cloud.

To finish we will dress a list of related issues that were not treated in detail in the present work:

- generalise to other (non Gaussian) wave functions
- generalise to a statistical ensemble of atoms
- quantify transit effects
- include other external fields (gravitational, inertial)
- apply to cylindrical microwave cavities

Some of the above points may prove essential for a complete understanding of the processes taking place in microwave frequency standards and more generally in all atom interferometry experiments. They are the subject of ongoing studies, the results of which will be presented in future publications.

Acknowledgements

Helpful discussions with C. Salomon, J. Fils, Y. Sortais are gratefully acknowledged. P.W. was supported for this work by CNES research grant 793/00/CNES/8201.

References

[1] Bordé C.J., *Quantum theory of clocks and gravitational sensors using atom interferometry*, in *Laser Spectroscopy*, Blatt R. et al. ed., World Scientific, (1999).
[2] Bordé C.J. et al., Phys. Rev. A **30**, 4, (1984), 1836; Ishikawa J. et al., Phys. Rev. A **49**, 6, (1994), 4794.
[3] Santarelli et al., PRL **82**, 23, (1999), 4619.
[4] Sortais et al., PRL **85**, 15, (2000), 3117.
[5] Lemonde P. et al., *Cold-Atom Clocks on Earth and in Space*, in *Frequency Measurement and Control*, Luiten A.N. ed., Springer (2001), 131.
[6] Udem T. et al., PRL **86**, 22, (2001), 4996.
[7] A. Peters, K.Y. Chung, S. Chu, Metrologia **38**, (2001), 25.
[8] Snadden M.J. et al., PRL **81**, 5, (1998), 971.
[9] Gustavson T.L., Landragin A., Kasevich M.A., Class. Quantum Grav. **17**, (2000), 1.
[10] Ramsey N.F., *Molecular Beams*, Oxford Univ. Press., (1956).
[11] Bordé C.J., *Matter wave interferometers: a synthetic approach*, in *Atom Interferometry*, P. Berman ed., Academic Press, (1997).
[12] Young B., Kasevich M., Chu S., *Precision atom interferometry with light pulses*, in *Atom Interferometry*, P. Berman ed., Academic Press, (1997).
[13] Cohen-Tannoudji C., Collège de France, cours 1993/1994, available at http://www.lkb.ens.fr/
[14] Bordé C.J., C.R.Acad. Sci. Paris, t.2, IV, (2001), 509.
[15] Storey P., Cohen-Tannoudji C., J. Phys. II France **4**, (1994), 1999-2027.
[16] Bordé C.J., *Propagation of laser beams and of atomic systems*, in *Fundamental systems in quantum optics*, J. Dalibard (ed.), Elsevier (1991).